BioMed

MDPI

Article

Enhancing Prostate and Bladder Cancer Treatment: Exploring the Synergistic Potential of Entecavir and 5-Fluorouracil Combinations

Tânia Lourenço [1,2,3], Lara Marques [1,2,4], Eduarda Ribeiro [1,2,5] and Nuno Vale [1,2,4,*]

[1] PerMed Research Group, Center for Health Technology and Services Research (CINTESIS), Rua Doutor Plácido da Costa, 4200-450 Porto, Portugal; taniadiaslourenco@hotmail.com (T.L.); lara.marques2010@hotmail.com (L.M.); eduardaprr@gmail.com (E.R.)
[2] CINTESIS@RISE, Faculty of Medicine, University of Porto, Alameda Professor Hernâni Monteiro, 4200-319 Porto, Portugal
[3] Faculty of Pharmacy, University of Porto, Rua Jorge Viterbo Ferreira, 228, 4050-313 Porto, Portugal
[4] Department of Community Medicine, Information and Health Decision Sciences (MEDCIDS), Faculty of Medicine, University of Porto, Rua Doutor Plácido da Costa, 4200-450 Porto, Portugal
[5] ICBAS—School of Medicine and Biomedical Sciences, University of Porto, Rua Jorge Viterbo Ferreira, 228, 4050-313 Porto, Portugal
* Correspondence: nunovale@med.up.pt; Tel.: +351-220426537

Abstract: Prostate and bladder cancer treatments have several challenges, including intense side effects and mechanisms of resistance. Thus, it is urgent to find drugs that can fill these gaps. For this purpose, Entecavir (ETV) was tested alone and in combination with 5-Fluorouracil (5-FU). Prior to this, a preliminary computational analysis was conducted to evaluate the combination of these two drugs. After exposing PC-3 and UM-UC-5 cells to the drugs, cell morphology was assessed using a microscope, while cell viability, proliferation, and cytotoxicity were evaluated using the MTT assay, and finally, the statistical analysis was performed. It was concluded that ETV showed significant cytotoxic effects in the PC-3 cells, and 5-FU, although not as effective as in other tumor types, it managed to inhibit the viability of the PC-3 cells. The combination of 5-FU with ETV after 72 h of exposure is an advantageous association, surpassing the results of each drug alone. In the UM-UC-5 cells, ETV alone did not produce the expected effect, neither did the combination. Nevertheless, repurposing ETV has proven to be an effective strategy in PC, especially through its combination with 5-FU.

Keywords: drug repurposing; prostate cancer; bladder cancer; entecavir; 5-fluorouracil; combination studies

Citation: Lourenço, T.; Marques, L.; Ribeiro, E.; Vale, N. Enhancing Prostate and Bladder Cancer Treatment: Exploring the Synergistic Potential of Entecavir and 5-Fluorouracil Combinations. *BioMed* **2024**, *4*, 185–202. https://doi.org/10.3390/biomed4020015

Academic Editor: Wolfgang Graier

Received: 18 March 2024
Revised: 6 June 2024
Accepted: 11 June 2024
Published: 14 June 2024

1. Introduction

Bladder cancer (BC) is the tenth most common cancer in the urinary tract and can be diagnosed through cystoscopy, urine cytology, and bladder ultrasound, and complemented by blood and urine tests, and staging evaluations such as abdominal, pelvic, and thoracic computed tomography [1,2]. Similar to prostate cancer (PC), urinary microRNAs, such as miR-21-5p, miR-141-3p, or miR-205-5p, are crucial in the diagnosis, prognosis, and treatment of urothelial cancers [3]. These biomarkers are useful not only for distinguishing between malignant and non-malignant tumors but also for assessing the disease aggressiveness and prognosis, as changes in microRNA expression are linked to tumor progression. Additionally, microRNAs can serve as therapeutic targets by repressing the tumor suppressor genes and oncogenes [3].

Standard BC treatments include surgery (cystectomy or transurethral resection), chemotherapy (cisplatin, gemcitabine, mitomycin, methotrexate, vinblastine, doxorubicin, epirubicin, valrubicin), radiotherapy, and immunotherapy (pembrolizumab, nivolumab, atezolizumab, avelumab), among others [1,4–6].

In turn, PC is one of the most common malignancies among men and, consequently, one of the main causes of death [7]. Diagnosis can be achieved through digital rectal examination (DRE), evaluation of prostate-specific antigen (PSA) levels, PSA density, and prostatic biopsy [8,9]. Moreover, prostate-specific membrane antigen positron emission tomography (PSMA-PET) is highlighted as a diagnostic and treatment planning tool that offers superior sensitivity and accuracy, as well as reduced radiation exposure [10]. Also, it emphasizes the importance of magnetic resonance imaging (MRI) in diagnosing and assessing the aggressiveness and staging of both PC and BC. MRI has become essential for establishing the Prostate Imaging Reporting and Data System (PI-RADS) and Vesical Imaging Reporting and Data System (VI-RADS) [9,11,12]. To develop personalized treatments for each patient, it is crucial to integrate the findings from PI-RADS and VI-RADS with biomarker analysis, thus applying the principles of precision medicine [9].

Standard PC treatments include surgery (prostatectomy or orchiectomy), chemotherapy (docetaxel, cabazitaxel, mitoxantrone, estramustine), radiation therapy (external radiotherapy or brachytherapy), immunotherapy (Sipuleucel-T), hormone therapy (LHRH agonists/antagonists, antiandrogens, androgen synthesis inhibitors), and targeted therapy (olaparib, rucaparib), among other options, all of which should be selected based on the patient's characteristics and the nature of the disease [13,14].

However, some cancer therapies, specifically chemotherapy, have limitations such as the intense side effects in patients and the development of resistance to treatment [15–20]. Thus, it becomes relevant to find drugs that can address these shortcomings. Instead of developing new molecules, repurposing existing drugs with potential anticancer mechanisms is highly pertinent. Within the group of antivirals, Entecavir (ETV, Scheme 1) stands out as a nucleoside guanosine analogue with activity against the polymerase of the hepatitis B virus. It is indicated as a first-line treatment for chronic hepatitis B and is marketed under the brand name Baraclude® (Bristol Myers Squibb, Princeton, NJ, USA) in tablets of 0.5 mg and 1 mg, as well as in an oral solution [21,22]. ETV stands out among other drugs due to its inhibition of the PARP-1 and KDM5B enzymes, which are overexpressed in BC and PC and associated with tumorigenesis, tumor progression, and therapeutic resistance. Additionally, ETV prevents hepatitis B virus reactivation in cancer patients undergoing immunotherapy, chemotherapy, and/or corticosteroids [23,24].

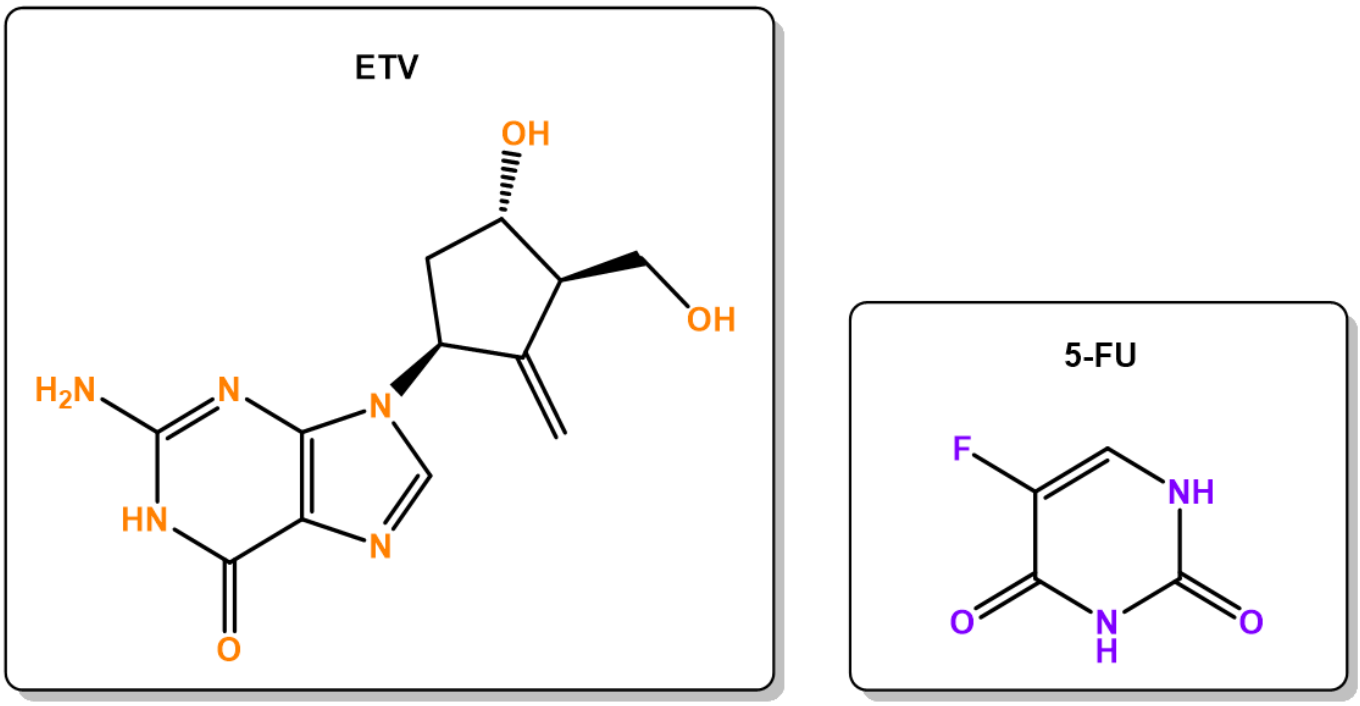

Scheme 1. Chemical structures of drugs Entecavir (ETV) and 5-Fluorouracil (5-FU).

Regarding 5-Fluorouracil (5-FU, Scheme 1), it is widely used for treating various cancers, including colorectal, gastric, breast, head and neck, esophageal, and pancreatic cancers. Some of the literature suggests its potential use in PC and BC; however, it is not a first-line treatment for both cancers [25]. Additionally, there are references indicating that 5-FU has radiosensitizing properties in prostate tumor cells and that its effect is enhanced by reducing folates, while PC overexpresses the prostate-specific membrane antigen (PSMA), which happens to be a folate hydrolase [26].

Interestingly, 5-FU remains one of the most used drugs in current chemotherapy regimens, despite its severe and frequent side effects [27,28]. Moreover, 5-FU is widely associated with the development of resistance, attributed to the presence of cancer stem cells, angiogenesis, tumor microenvironment, alterations in influx and efflux, mutations in target genes, and the overexpression of cell adhesion molecules, such as nectin-4 [29].

Therefore, to minimize the severe side effects and resistance associated with 5-FU and to increase its therapeutic efficacy, previous studies have explored combining ETV and 5-FU. Notwithstanding, the pharmacological interaction between two drugs, or drug–drug interaction (DDI), may indirectly contribute to synergistic effects, particularly regarding the increased intracellular concentrations [30]. A DDI occurs when two or more drugs interact, leading to changes in the effectiveness and toxicity of drugs.

Hence, this study aimed to further investigate the effects of ETV and 5-FU in the treatment of PC and BC. Initially, to evaluate the safety of combining ETV and 5-FU, we employed a computational approach to predict potential interactions, focusing on both metabolism- and transporter-mediated pathways between the two drugs. Subsequently, we investigated the individual and combined effects of ETV and 5-FU on the viability of the PC-3 and UM-UC-5 cell lines, to try and demonstrate the enhanced efficacy of combination over individual drug treatments.

2. Materials and Methods

2.1. Computational Modeling of ADMET Properties

The physicochemical and ADMET properties of both ETV and 5-FU were determined through in silico modeling using ADMET Predictor® (Version 10.4; SimulationPlus Inc., Lancaster, CA, USA). The chemical structures of ETV and 5-FU were drawn using MedChem Designer (Version 5.5; SimulationPlus Inc., Lancaster, CA, USA) and subsequently input into ADMET Predictor®. Parameters such as Log P, molecular weight, solubility, CYP-mediated metabolism, and drug transporters were estimated using this software tool.

2.2. Cell Culture and Reagents

The culture medium used was Dulbecco's Modified Eagle's Medium (DMEM) supplemented with a 1% solution of penicillin-streptomycin and 10% fetal bovine serum (FBS), acquired from Millipore Sigma (Merck KGaA, Darmstadt, Germany), along with phosphate-buffered saline (PBS) and dimethyl sulfoxide (DMSO). The 0.25% trypsin/ethylenediaminetetraacetic acid (EDTA) solution and trypan blue were obtained from Gibco (Thermo Fisher Scientific, Inc., Waltham, MA, USA). The ETV and 5-FU drugs, as well as the tetrazolium-based colorimetric assay agent (MTT), were acquired from Sigma-Aldrich (Merck, Algés, Portugal).

The cells were purchased from the American Type Culture Collection (ATCC, Manassas, VA, USA), and maintained in an incubator at 37 °C with 5% carbon dioxide in DMEM supplemented with a 1% solution of penicillin-streptomycin and 10% FBS. The culture medium was replaced twice a week, with one replacement coinciding with cell splitting. All procedures were conducted in a vertical laminar flow hood using sterilized materials.

2.3. Cell Seeding

In achieving cell confluence (at approximately 75–80%), the culture medium was first removed, followed by a wash with PBS and further removal via aspiration. Subsequently, cells on the flask wall were detached through trypsinization using a 0.25% trypsin/EDTA

solution. The cells were then incubated for 5 min at 37 °C in a 5% carbon dioxide atmosphere. Following this, the trypsin effect was neutralized by adding culture medium, and the resulting cell suspension was centrifuged for 5 min at 1100 rotations per minute (rpm). The supernatant was then replaced with fresh culture medium, and the cells were resuspended.

Next, viable cell counting was performed using trypan blue, a stain exclusively targeting cells with compromised cell membranes. This process was performed using a Neubauer chamber and the Leica DMI 6000B microscope equipped with a Leica DFC350 FX camera (Leica Microsystems, Wetzlar, Germany).

2.4. Cell Treatment

For the PC-3 cells, the cytotoxicity of ETV alone was evaluated after 24 h, 48 h, and 72 h, using the drug concentrations of 0.01, 0.1, 1, 10, 25, 50, and 100 μM. Meanwhile, the evaluation of 5-FU alone was conducted only after 48 h, also using the drug concentrations of 0.01, 0.1, 1, 10, 25, 50, and 100 μM. Additionally, the IC_{50} of 5-FU was determined after 48 h. Concerning the combination studies, the IC_{50} of 5-FU for 48 h in combination with ETV at the concentrations of 0.01, 0.1, 1, 10, 25, 50, and 100 μM was analyzed after 24 h, 48 h, and 72 h, with exposure to both drugs conducted simultaneously.

For the UM-UC-5 cells, the cytotoxicity of ETV alone was also evaluated after 24 h, 48 h, and 72 h, using the drug concentrations of 0.01, 0.1, 1, 10, 25, 50, and 100 μM. Fortunately, 5-FU was previously tested in the UM-UC-5 cell line by our research team, enabling us to obtain an IC_{50} of 13.41 μM [31]. Concerning the combination studies, the IC_{50} of 5-FU in combination with ETV at the concentrations of 0.01, 0.1, 1, 10, 25, 50, and 100 μM was analyzed after 24 h, 48 h, and 72 h, with exposure to both drugs conducted simultaneously.

Regarding the control cells, these were exposed to a concentration of 0.1% DMSO. Furthermore, DMSO was also used to dissolve ETV and 5-FU.

2.5. Morphological Analysis

The morphological assessments of the PC-3 and UM-UC-5 cells were conducted after the determined exposure time for each experiment using a Leica DMI 6000B microscope equipped with a Leica DFC350 FX camera, and the images were captured using the Leica LAS X software (v3.7.4) (Leica Microsystems, Wetzlar, Germany).

2.6. MTT Assay

The MTT colorimetric assay was employed to evaluate cellular viability, proliferation, and cytotoxicity. This method assesses cell viability after drug treatment in comparison to control cells. It measures the mitochondrial function of the PC-3 and UM-UC-5 cells; hence, if the mitochondria are functional, MTT is reduced by the mitochondrial dehydrogenases, forming formazan crystals which present a purple-colored product. The more intense the color in each well, the higher the cellular viability and, consequently, the higher the absorbance value [32].

The MTT assay was conducted in the absence of light, involving the removal of the culture medium from the wells after the defined time for drug action. Subsequently, 100 μL of MTT solution (0.5 mg/mL in PBS) was added to each well of the plate, followed by a 2 h incubation at 37 °C and 5% carbon dioxide, allowing for the formation of formazan crystals. After this period, MTT was removed and 100 μL of DMSO was added to each well to solubilize the formazan crystals. The plate was then placed in an automatic plate reader (Tecan Infinite M200, Tecan Group Ltd., Männedorf, Switzerland) for agitation and measurement of absorbance at 570 nm.

2.7. Statistical Analysis

GraphPad Prism 9 software (GraphPad Software Inc., San Diego, CA, USA) was used to generate cell viability graphs, with the results presented as mean cell viability ± SEM. To compare the control group with the experimental group for each concentration of

individually studied drugs, a one-way ANOVA test was utilized employing Dunnett's multiple comparisons method. Regarding the PC-3 cells' combination studies, a two-way ANOVA test was used to compare the combination results with the results of each drug alone at their respective concentrations.

Statistical significance was established for values at $p < 0.05$ and represented as *, **, ***, and **** to indicate $p < 0.05$, $p < 0.01$, $p < 0.001$, and $p < 0.0001$, respectively. The brackets above the bar graphs represent the comparisons made between the bars to analyze statistical significance.

The IC_{50} was obtained using the same software, based on the generated dose–response curves.

3. Results

3.1. Pharmacokinetic Evaluation of the Combination of 5-FU and ETV

A preliminary analysis using a computational approach was performed to evaluate the combination of 5-FU and ETV. The physicochemical properties of both drugs were estimated by ADMET Predictor® (Table 1). A comparison of these attributes was conducted against values from prominent drug databases and those obtained from other ADME properties predictive platforms, namely SwissADME and pkSCM (optimized values). As noted, the simulated data are rather considerable.

Table 1. Predicted and optimized physicochemical properties of 5-FU and ETV.

Drug	Physicochemical Properties	Predicted Value	Optimized Value	Reference
5-FU	LogP	−0.783	−0.798	[33]
	pKa	11.08	8.02	[34]
	Molecular Weight (g/mol)	130.08	130.08	[33,35]
	Water Solubility (mg/mL)	11.46	5.86	[34]
	Diff. Coeff. ($cm^2/s \cdot 10^5$)	1.462	ND	ND
	Peff ($cm/s \cdot 10^4$)	2.705	ND	ND
	BBB penetration	High	Low	[35]
ETV	LogP	−1.076	−0.823	[33,35,36]
	pKa	9.59	12.00	[36]
	Molecular Weight (g/mol)	277.28	277.28	[33,35,36]
	Water Solubility (mg/mL)	2.065	2.400	[36]
	Diff. Coeff. ($cm^2/s \cdot 10^5$)	0.842	ND	ND
	Peff	0.321	ND	ND
	BBB penetration	Low	Low	[35]

pKa, ionization constant; Diff. Coeff, differential coefficient; Peff, effective human jejunal permeability; BBB, blood–brain barrier; ND, not defined.

The metabolic profiles of 5-FU and ETV were thoroughly examined using the ADMET Predictor® to evaluate metabolism-mediated DDIs. The analysis revealed that the phase I metabolic reactions of 5-FU involve the active participation of CYP1A2, CYP2A6, and CYP2E1 enzymes (Table 2). Notably, the software predicted the substrate-associated precision for CYP2A6 and CYP2E1 to be less than 50%, which raises questions about the reliability of these predictions. Conversely, a potential inhibitory effect of 5-FU on CYP2B6 is observed. However, the associated uncertainty in this prediction is high as well. ETV acts as a substrate for the CYP3A4 enzyme, with a precision of 72%. Furthermore, the software indicated a potential inhibitory effect of ETV on CYP2B6, yet the certainty of this prediction is less than 50%.

Table 2. Metabolic profile of drugs 5-FU and ETV.

Drug	CYP Enzyme	Inhibitor	Substrate	Km	V_{max}	CL	Sites of Metabolism
5-FU	1A2	No (96%)	Yes (91%)	3193.026	1.620	0.026	C6
	2A6	No (93%)	Yes (42%)	ND	ND	ND	ND
	2B6	Yes (% ND)	No (98%)	NS	NS	NS	NS
	2C8	No (97%)	No (94%)	NS	NS	NS	NS
	2C9	No (97%)	No (75%)	NS	NS	NS	NS
	2C19	No (96%)	No (81%)	NS	NS	NS	NS
	2D6	No (97%)	No (84%)	NS	NS	NS	NS
	2E1	No (% ND)	Yes (43%)	ND	ND	ND	ND
	3A4	No (96%)	No (83%)	NS	NS	NS	NS
ETV	1A2	No (96%)	No (72%)	NS	NS	NS	NS
	2A6	No (99%)	No (98%)	NS	NS	NS	NS
	2B6	Yes (44%)	No (98%)	NS	NS	NS	NS
	2C8	No (88%)	No (98%)	NS	NS	NS	NS
	2C9	No (97%)	No (99%)	NS	NS	NS	NS
	2C19	No (96%)	No (95%)	NS	NS	NS	NS
	2D6	No (97%)	No (95%)	NS	NS	NS	NS
	2E1	No (89%)	No (98%)	NS	NS	NS	NS
	3A4	No (96%)	Yes (72%)	82.119	100.244	135.499	C6, C3, C2, N19, C5

ND, not defined; NS, no substrate. The CYP enzymes for which the compounds are substrate are highlighted in yellow.

Drug transporters are also recognized as crucial determinants of drug disposition and toxicity by affecting the ADME of drugs. The key transporters involved in DDIs include P-glycoprotein (Pgp), Breast Cancer Resistance Protein (BCRP), Organic Anion Transporting Polypeptide 1B1 (OAT1PB1), Organic Anion Transporter 1 (OAT1), Organic Anion Transporter 3 (OAT3), and Organic Cation Transporter 2 (OCT2). Understanding whether ETV and 5-FU act as the substrates or inhibitors of these drug transporters could potentially explain an interaction between the two drugs. Therefore, we also used ADMET Predictor® to estimate their role (Table 3). Accordingly, ETV and 5-FU are both substrates of Pgp, BCRP, OAT1, OAT3, and OCT2, with high estimation precision.

Table 3. Transporter–drug interaction profile of ETV and 5-FU.

Drug Transporter	Drug	Inhibitor	Substrate
Pgp	5-FU	No (93%)	Yes (83%)
	ETV	No (93%)	Yes (99%)
BCRP	5-FU	No (96%)	Yes (88%)
	ETV	No (96%)	Yes (98%)
OATP1B1	5-FU	No (79%)	No (98%)
	ETV	No (79%)	No (98%)
OATP1B3	5-FU	No (92%)	No (96%)
	ETV	Yes (72%)	No (96%)
OAT1	5-FU	No (98%)	Yes (98%)
	ETV	No (98%)	Yes (67%)
OAT3	5-FU	No (95%)	Yes (59%)
	ETV	No (95%)	Yes (99%)
OCT2	5-FU	No (99%)	Yes (75%)
	ETV	No (99%)	Yes (95%)

Pgp, P-glycoprotein; BCRP, Breast Cancer Resistance Protein, OATP1B1, Organic anion transporting polypeptides 1B1; OATP1B3, Organic anion transporting polypeptides 1B3; OAT1, Organic anion transporter 1; OAT3, Organic anion transporter 3; OCT2, Organic cation transporter 2.

3.2. PC-3 Cells

3.2.1. Cytotoxicity of 5-FU

The efficacy of 5-FU alone in the treatment of PC (PC-3 cells) was evaluated at the concentrations of 0.01, 0.1, 1, 10, 25, 50, and 100 μM over 48 h. This study was conducted in three independent experiments, each with $n = 3$. Hence, the results of the cell viability and morphological assessment of 5-FU tested alone are depicted in Figure 1 and Supplementary Figure S1, respectively. It can be observed that after 48 h, 5-FU significantly reduces the cell viability of the PC-3 cells. Overall, cell viability is lower at higher drug concentrations, and concentrations equal to or greater than 10 μM are associated with lower cell viability, while concentrations equal to or greater than 25 μM can decrease cell viability to around 50%.

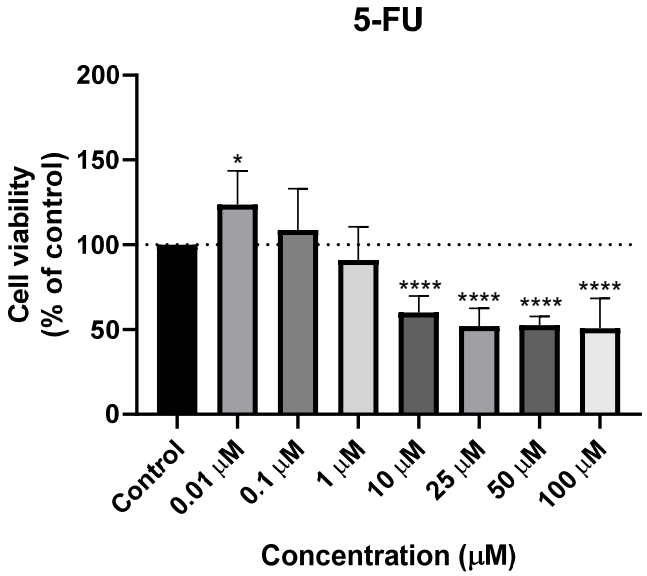

Figure 1. Cell viability results of the PC-3 cells after exposure to increasing concentrations of 5-FU (0.01–100 μM) for 48 h. Cell viability reflects the cytotoxicity of 5-FU and was determined using the MTT assay, where control cells were treated with 0.1% DMSO (vehicle). The results are presented as mean ± SEM. * Statistically significant vs. control (vehicle) at $p < 0.05$; **** Statistically significant vs. control (vehicle) at $p < 0.0001$.

The IC_{50} corresponds to the concentration required to inhibit cell viability by 50% and was obtained through the dose–response curve for 48 h, yielding a value of 3.22 μM. Comparatively, this value is considerably low in contrast to the results of the cell viability bar graph (Figure 1), where cell viability reaches approximately 50% only with concentrations equal to or greater than 25 μM of 5-FU.

Thus, 5-FU causes a reduction in cell viability in the PC-3 cells, especially at higher concentrations, although it seems to have less cytotoxic activity in PC than in tumors, where it is used as a first-line treatment.

3.2.2. Cytotoxicity of ETV

ETV was the repurposed drug tested on the PC-3 cells, evaluating its efficacy alone in the treatment of PC at the concentrations of 0.01, 0.1, 1, 10, 25, 50, and 100 μM over 24, 48, and 72 h. The results of the morphological assessment of ETV are represented in Supplementary Figure S2 and to avoid redundant information, the cell viability bar graphs for ETV alone will be presented later in the next topic, where they will serve as a comparison to the those of the combination studies.

3.2.3. Cytotoxicity of Combination Studies

After testing each drug individually, combinations of 5-FU and ETV were evaluated. The IC_{50} of 5-FU obtained in the 48 h studies (3.22 µM) was tested with all the concentrations of ETV (0.01–100 µM) for 24, 48, and 72 h, with both drugs being added simultaneously. The results of the morphological assessment and cell viability are presented in Supplementary Figure S3 and Figure 2, respectively. Combining the IC_{50} value of 5-FU obtained in the 48 h study (3.22 µM) with the increasing concentrations of ETV (0.01–100 µM) that were added simultaneously for 24 h did not show a direct relationship between the increasing ETV dosages and decreased cell viability (Figure 2—24 h). However, in the 48 h study, a slight relationship between the increasing ETV dose and decreased cell viability was observed (Figure 2—48 h). It is in the 72 h study that it becomes evident that combining the IC_{50} value of 5-FU obtained in the 48 h study (3.22 µM) with the increasing concentrations of ETV (0.01–100 µM) added simultaneously yields better results than the drugs alone (Figure 2—72 h). There appears to be a relationship with the time factor, as the results of the 72 h study were superior to the others. Notably, in the 72 h study, the 50 µM concentration of ETV exhibits a cytotoxic effect superior to the IC_{50} of 5-FU, and when combined, they are more effective than when tested alone. This suggests that ETV contributed significantly to the effect (Figure 3).

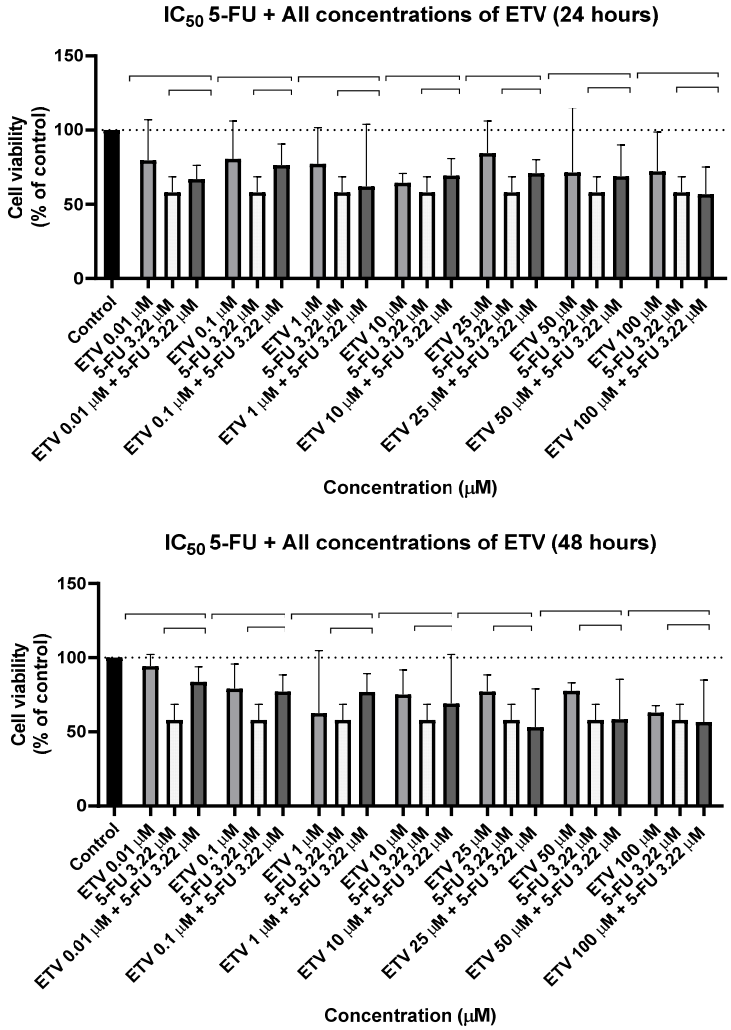

Figure 2. *Cont.*

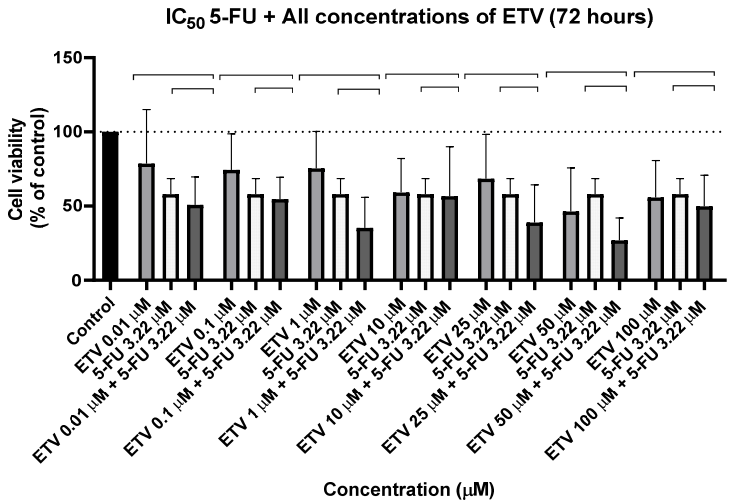

Figure 2. Cytotoxic effects on the PC-3 cell line after exposure to the combination of the IC_{50} value of 5-FU (3.22 μM) with increasing concentrations of ETV (0.01–100 μM) added simultaneously and evaluated after 24, 48, and 72 h. Control cells were treated with a concentration of 0.1% DMSO (vehicle), cell viability was determined using the MTT assay, and the results are presented as mean ± SEM.

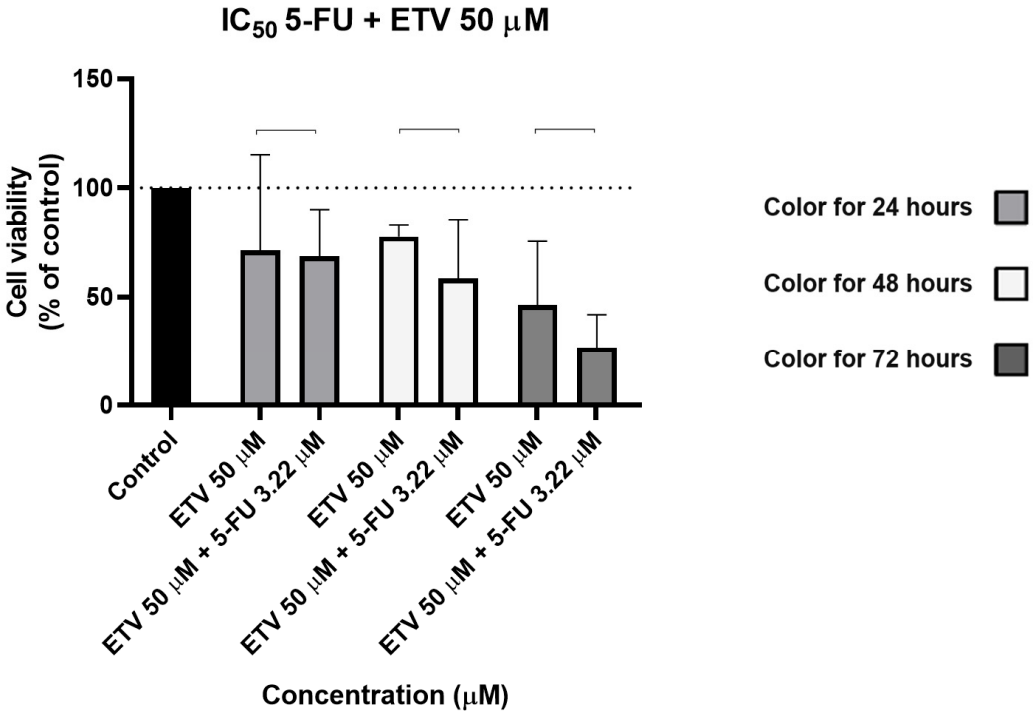

Figure 3. Cytotoxic effects on the PC-3 cell line after exposure to the combination of the IC_{50} value of 5-FU (3.22 μM) with 50 μM of ETV added simultaneously and evaluated after 24 h (light gray), 48 h (white), and 72 h (dark gray), compared to 50 μM of ETV for the same time periods. Control cells were treated with a concentration of 0.1% DMSO (vehicle), cell viability was determined using the MTT assay, and the results are presented as mean ± SEM.

3.3. UM-UC-5 Cells

3.3.1. Cytotoxicity of ETV

ETV was tested on the UM-UC-5 cells, evaluating its efficacy alone in the treatment of BC at the concentrations of 0.01, 0.1, 1, 10, 25, 50, and 100 μM over three time periods (24, 48, and 72 h). The results of the cell viability and morphological assessment when ETV was tested alone are represented in Figure 4 and Supplementary Figure S4, respectively. It

can be observed that ETV did not decrease the cell viability of the UM-UC-5 cells at all the tested concentrations and time points, except only very slightly in the 72 h study, which was not significant.

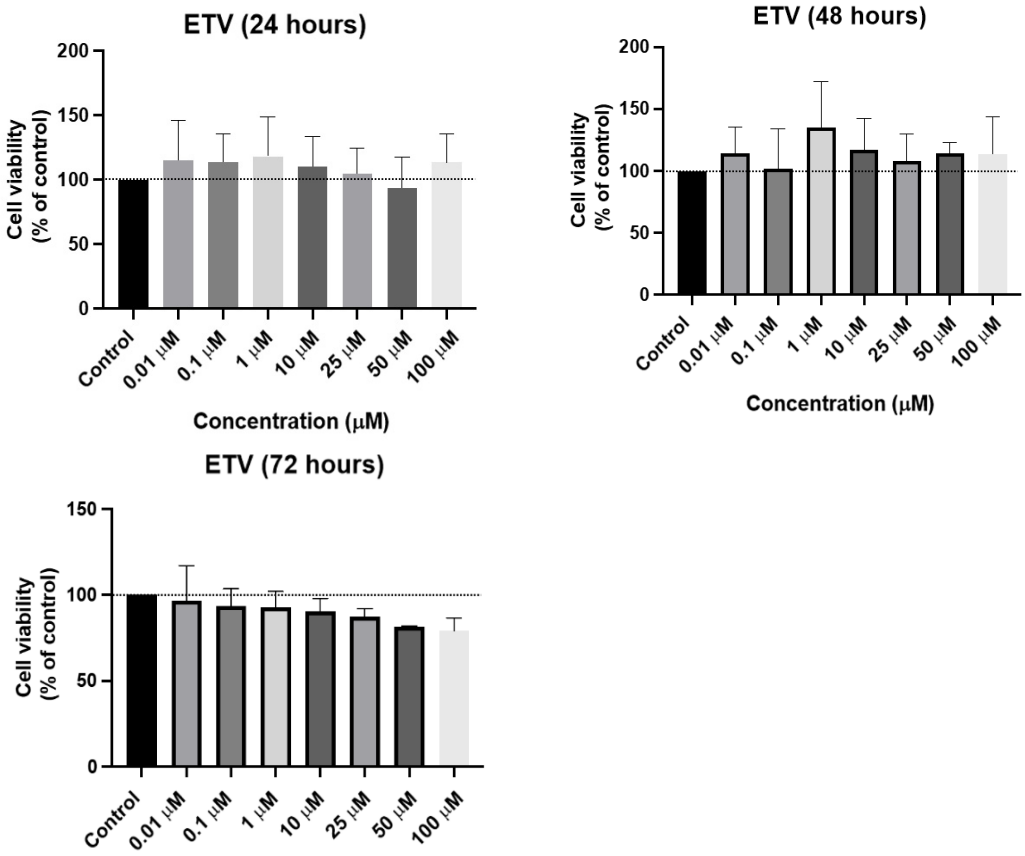

Figure 4. Cell viability results of the UM-UC-5 cells after exposure to increasing concentrations of ETV (0.01–100 μM) for 24, 48, and 72 h. Cell viability reflects the lack of cytotoxicity of ETV and was determined using the MTT assay, where control cells were treated with 0.1% DMSO (vehicle). The results are presented as mean ± SEM.

3.3.2. Cytotoxicity of Combination Studies

After testing each drug individually, combinations of 5-FU and ETV were evaluated. However, it is important to mention that 5-FU was previously tested in the UM-UC-5 cell line by our research team, enabling us to obtain an IC_{50} of 13.41 μM [31].

The IC_{50} of 5-FU was tested with all the concentrations of ETV (0.01–100 μM) for 24, 48, and 72 h, with both drugs being added simultaneously. The results of the morphological assessment and cell viability are presented in Supplementary Figure S5 and Figure 5, respectively. Combining the IC_{50} value of 5-FU (13.41 μM) with increasing concentrations of ETV (0.01–100 μM) added simultaneously for 24 h did not decrease the cell viability of the UM-UC-5 cells. However, in the 48 h study, and particularly in the 72 h study, a decrease in cell viability was observed, specifically in the combinations of IC_{50} 5-FU with 0.01 μM ETV, as well as IC_{50} 5-FU with 0.1 μM of ETV.

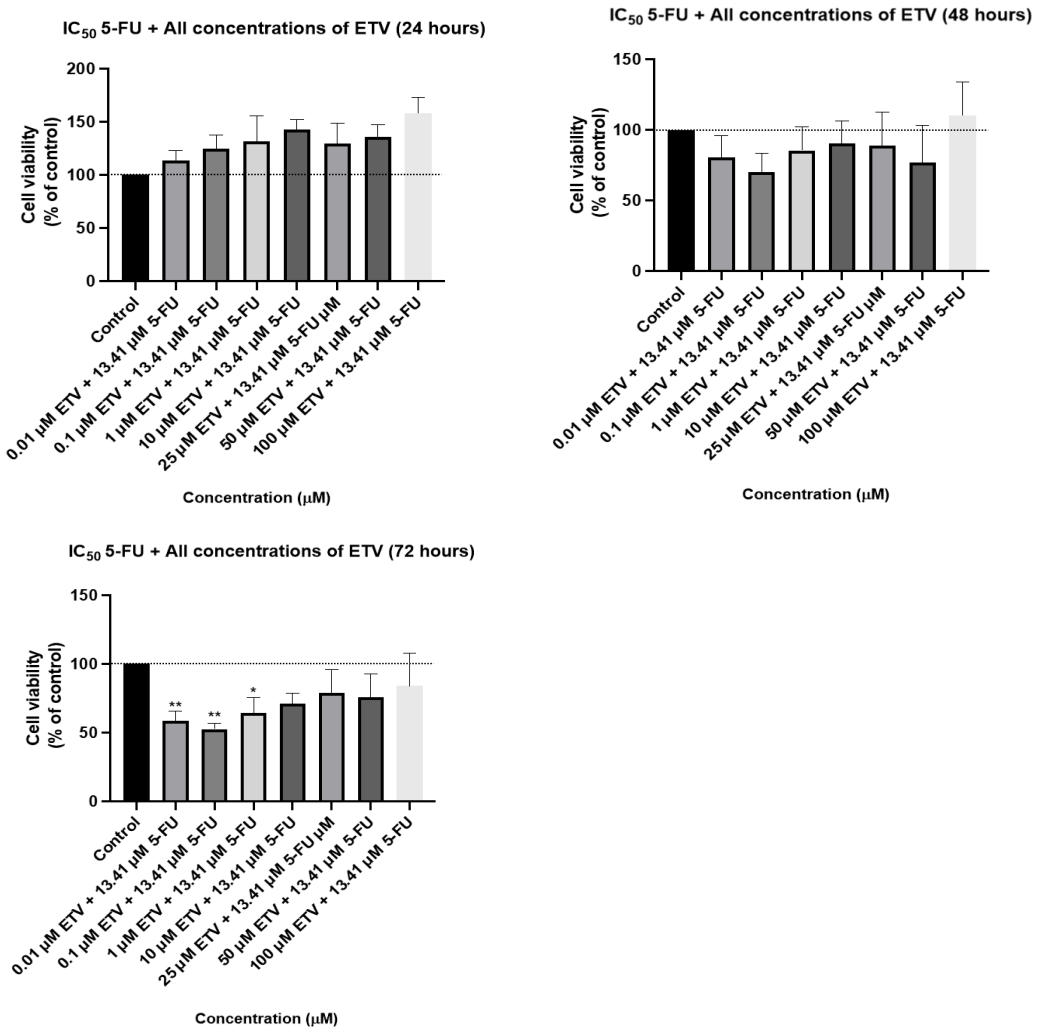

Figure 5. Cytotoxic effects on the UM-UC-5 cell line after exposure to the combination of the IC_{50} value of 5-FU (13.41 µM) with increasing concentrations of ETV (0.01–100 µM) added simultaneously and evaluated after 24, 48, and 72 h. Control cells were treated with a concentration of 0.1% DMSO (vehicle), cell viability was determined using the MTT assay, and the results are presented as mean ± SEM. * Statistically significant vs. control (vehicle) at $p < 0.05$; ** Statistically significant vs. control (vehicle) at $p < 0.01$.

4. Discussion

Considering that ETV has shown promise in PC and BC treatment and has been relatively understudied for this purpose, it was selected as the repurposed drug for this study, with 5-FU chosen as the reference drug. The rationale behind combining repurposed drugs with antineoplastic drugs is to achieve better therapeutic outcomes than those achieved individually, although this approach may pose challenges such as unexpected side effects or diminished clinical efficacy.

In this study, we aimed to assess whether ETV and 5-FU reduced the viability of the PC-3 and UM-UC-5 cell lines when tested individually and to test them in combination and evaluate their potential efficacy in PC and BC treatment.

Therefore, we first analyzed the potential for an interaction between the drugs to be tested, since DDIs can indirectly contribute to a synergistic effect between co-administered drugs, particularly through alterations in pharmacokinetic (PK) or pharmacodynamic (PD) profiles. The altered function of the cytochrome P450 (CYP) enzymes or drug transporters is the most commonly documented PK interaction [37–39]. CYP enzymes are a superfamily of monooxygenases that play a crucial role in the oxidative metabolism of a wide range

of drugs [40]. Transporter-mediated DDIs occur when one drug affects the function of transport proteins, altering the absorption, distribution, or elimination (ADME) of another drug. Transport proteins are crucial in the body's defense mechanism as they help in the uptake and efflux of endogenous and exogenous substances, including drugs [41]. The modulation of metabolic enzymes and drug transporters plays a central role in DDIs since it can significantly affect the safety and effectiveness of drug therapy.

The significance of CYP enzymes in metabolism-mediated DDIs is well documented. They can be inhibited or induced by various drugs, leading to changes in the metabolic clearance of co-administered drugs. Multiple mechanisms of inhibition and induction of CYP enzymes have been elucidated [42]. Similar to how drugs can compete for protein-binding sites, they can also compete for enzyme catalytic sites. This competition for the same enzyme can inhibit or induce drug metabolism, posing the risk of undesirable elevations in plasma drug concentrations. For instance, if a drug strongly inhibits a CYP enzyme that is responsible for the metabolism of a second drug, its co-administration could result in increased levels of the second drug, potentially leading to toxic effects.

Within this framework, changes in the ADME processes can significantly impact intracellular concentrations at the therapeutic target, shaping the combined therapeutic outcome. Therefore, we initially sought to understand whether ETV and 5-FU interact with each other when administered concurrently so as to explain the rationale behind their combined use. Our approach involved ADMET Predictor®, a machine-learning (ML) software tool that quickly and accurately predicts several properties of compounds. This comprehensive approach aimed to provide a basis for subsequent in vitro experiments.

Our results have demonstrated that 5-FU could be metabolized by CYP1A2, CYP2A6, and CYP2E1. However, the software's prediction accuracy for these enzymes (below 50%) raises questions about their involvement in the 5-FU metabolism. In fact, 5-FU is primarily metabolized by enzymes involved in nucleotide metabolism, contributing to its anticancer effects [43]. Moreover, a study conducted by Park et al. [44], showing little or no inhibitory effect of 5-FU on CYP enzymes, stated that DDIs between the co-administered drugs and 5-FU are not related to CYP inhibition. ETV, in turn, was identified as a potential substrate of CYP3A4, with 72% accuracy, which contradicts the existing literature [36]. Considering this inconsistency with the reported scientific knowledge, we believe that these predictions should be validated with experimental data to confirm the role of these enzymes in the metabolism of 5-FU and ETV. Despite this, assuming neither drug acts as an inhibitor nor substrate of the CYP450 enzyme system, we may conclude that metabolism-mediated DDIs are very unlikely.

Nevertheless, other mechanisms underlying DDIs are acknowledged. As plasma membrane transporters are responsible for either the uptake of substances into cells or the efflux out of cells, drug transporters significantly impact the drug disposition processes [41,45]. The interaction between drugs and transport proteins, known as a transporter-mediated DDI, occurs when a drug affects the function of these proteins. Thus, inhibition or induction by one drug can lead to an increase or decrease in serum or tissue concentrations of another drug utilizing the same pathway when administered simultaneously. Bearing this in mind, we conducted an analysis of the profiles of ETV and 5-FU concerning their roles as inhibitors/substrates of specific membrane proteins.

The software predicted that 5-FU and ETV are both substrates of Pgp, BCRP, OAT1, OAT3, and OCT2. Regarding 5-FU, there is no clear evidence indicating that this chemotherapeutic agent is a substrate of these drug transporters. The interaction between these transporters and 5-FU needs further investigation. On the other hand, some studies have reported that ETV is a substrate of BCRP, OAT1, and OAT3 [46,47]. Furthermore, there is no clear evidence indicating that ETV is a substrate of Pgp and OCT2. In fact, Mandíková et al. [48] conducted an in vitro study to investigate the potential of ETV to interact with SLC transporters, and their results did not detect a significant interaction between ETV and OCT2.

When two drugs share the same transporter as substrates and are co-administered, they may compete for the same binding sites on the transporter. This competition has

the potential to induce changes in the PK of one or both drugs. Hence, considering our prediction, we can infer that these drugs use common cell transporters, establishing the potential for interactions at this level. The interaction between ETV and 5-FU could then result in enhanced cytotoxic activity in tumor cells since the anti-tumor effect of 5-FU may be evidenced with the combination of 5-FU-ETV. Although computational tools provide valuable insights into DDIs, these findings should be validated with in vitro experiments.

Therefore, cell viability following exposure to all drugs was obtained using the MTT assay. Regarding the PC-3 cells, concentrations of 0.01, 0.1, 1, 10, 25, 50, and 100 μM of ETV alone were tested after 48 h, and the IC_{50} value was determined through the 48 h dose–response curve, which was found to be 0.06 μM. After establishing that ETV reduced PC-3 cell viability in 48 h, assays were conducted for 24 and 72 h with increasing concentrations of ETV (0.01–100 μM) to assess potential time-dependent influences on cell viability. Consequently, it was observed that ETV reduced cell viability at all concentrations tested over 24, 48, and 72 h, albeit with a clear time-dependent effect, which is also corroborated by the images from the morphological studies; cell viability significantly decreased after 72 h, and was particularly evident with 50 μM of ETV, reaching cell viability levels of below 50%.

The ETV IC_{50} obtained for 48 h was 0.06 μM, which, when compared to the bar graph results of cell viability, appears remarkably low. This could be explained by the IC_{50} being calculated via the dose–response curve, a mathematical projection obtained through our experimental results and aimed at determining the concentration required to inhibit 50% of tumor cell viability. Ideally, lower IC_{50} values suggest that the drug is effective at lower concentrations, resulting in reduced toxicity when administered. However, the IC_{50} value is an estimation, despite having been obtained through our experimental results, that may not fully align with the actual biological responses and, consequently, the real cell viability values [49,50]. The literature suggests that for hepatitis B virus inhibition in vitro, ETV IC_{50} values range from 0.36 nM to 3.6 nM [51]. In this study, however, the IC_{50} for the PC-3 cells was considerably higher, potentially indicating that higher ETV concentrations are needed to inhibit prostate tumor cells compared to inhibiting the hepatitis B virus.

Indeed, there are no published in vitro tests where ETV has been tested on the PC-3 cells, making this a pioneering study that supports available theoretical information in the literature. Thus, ETV exhibits cytotoxic effects on PC cell lines, an effect that may be attributed to various mechanisms of action still requiring confirmation, such as the inhibition of KDM5B, the PI3K/AKT signaling pathway, and/or PARP-1. It would be pertinent to understand some characteristics of the PC-3 cells used in this study to discern the mechanism behind their cytotoxic effect, specifically KDM5B expression and BRCA1 and BRCA2 gene expression. Interest in BRCA1 and BRCA2 gene expression has arisen from the need to understand if ETV is indeed a PARP inhibitor. PARP inhibitors function on the principle of synthetic lethality, requiring the functional loss of two genes to trigger cell death. Therefore, only patients with mutations in BRCA genes or with BRCAness tumors would benefit from ETV therapy for PC, as inhibiting PARP in the cells with BRCA mutations renders them unable to repair DNA damage, leading to error accumulation and consequent cell death [52,53]. As a PARP inhibitor, ETV may inhibit the repair of DNA damage, particularly in cancer stem cells, and irreparable damage to these cells will ultimately lead to apoptosis.

Regarding 5-FU, the concentrations of 0.01, 0.1, 1, 10, 25, 50, and 100 μM were tested after 48 h, yielding an IC_{50} value through the dose–response curve of 3.22 μM. This value was validated by another study testing the 48 h IC_{50} independently and confirming that the PC-3 cell viability had reduced to approximately 50%. The IC_{50} of 3.22 μM for 5-FU aligns with the range of IC_{50} capable of inhibiting the in vitro proliferation of various human tumor cell lines described in the literature (3.18 μM to 17.7 μM), although these values are not specific to the PC-3 cells [54].

However, unlike ETV, which reduced cell viability at all the tested concentrations, 5-FU only demonstrated this effect at concentrations equal to or greater than 1 μM, according

to the bar graph and the images from morphological studies. Notably, in Supplementary Figure S1, there are morphological variations between experiments of the same concentrations, including in the control group. However, the fact that three experiments were carried out increases the representativeness of the study.

Nonetheless, a relationship between increased 5-FU concentration and reduced cell viability could be established, with concentrations between 25 and 100 μM reducing cell viability to approximately 50%. Although 5-FU did not exhibit a pronounced reduction in cell viability as in other cancer cell lines, it demonstrated significant cytotoxicity in the PC-3 cells, warranting further combination studies. However, it is pertinent to mention that due to its radiosensitizing ability, higher levels of cytotoxicity might be achieved if radiation were applied to the PC-3 cells [28].

Still regarding the PC-3 cells, combination studies were conducted to test the IC_{50} of 5-FU (3.22 μM) with increasing concentrations of ETV (0.01–100 μM) for 24, 48, and 72 h. The objective was to assess whether the combination of 5-FU with ETV was more cytotoxic compared to the drugs used individually.

In the 24 h study, the cytotoxicity of the combination was lower than the IC_{50} cytotoxicity. When comparing ETV + 5-FU with ETV alone, the combination of drugs was more effective, except at 10 μM of ETV. Notably, 3.22 μM of 5-FU reduced cell viability more than all the ETV concentrations and the combinations (except IC_{50} of 5-FU with 100 μM of ETV). Similarly, in the 48 h study, using both drugs revealed lower cytotoxicity than the IC_{50} of 5-FU, despite being more cytotoxic than ETV alone (except for 1 μM of ETV). In this study, a relationship between increased ETV concentration and reduced cell viability of the combination with 5-FU was observed at concentrations ranging from 0.01 to 25 μM of ETV. Furthermore, the IC_{50} of 5-FU also reduced cell viability more than all the ETV concentrations and the combinations (except IC_{50} of 5-FU with 25 and 100 μM of ETV). In the 72 h study, the combination of ETV and 5-FU demonstrated significant cytotoxicity in comparison with the IC_{50} of 5-FU and ETV alone. However, unlike what was expected, there was no relationship between the increased ETV concentrations and cell viability. The 3.22 μM of 5-FU reduced cell viability more than the ETV concentrations (except 50 and 100 μM). On the other hand, the 72 h combination showed higher cytotoxicity than 3.22 μM of 5-FU.

When comparing the cytotoxic effects of 3.22 μM of 5-FU and 50 μM of ETV for 24, 48, and 72 h, the crucial role of time becomes evident. It confirms that for the 72 h period, the combination of 5-FU with ETV induces more cytotoxicity than the drugs used individually—which did not occur for 24 and 48 h. Contrary to our expectations, the cell viability at 50 μM of ETV for 48 h was not lower than for 24 h.

Therefore, the best result obtained in this entire study (the one that induced the most cytotoxicity in the PC-3 cells) was the combination of 5-FU with 50 μM of ETV for 72 h, indicating an added value in combining these two drugs, likely due to their synergistic effect—where the combination of two drugs produces an effect greater than the sum of their individual effects. Thus, one of the significant advantages of synergistic effects is the possibility of reducing individual doses of the two drugs used compared to their individual use, thereby optimizing therapy, decreasing the likelihood of severe side effects, and finally, increasing the treatment success rate. Moreover, the different mechanisms of action of the drugs involved allow for a delay in the development of resistance to treatments [20,55]. However, more studies are needed to corroborate this theory about synergistic effects. Another hypothesis to account for the observed synergistic effect involves the potential interaction between the two drugs at the transporter level, specifically Pgp and BCRP. These transmembrane proteins are frequently implicated in chemotherapeutic resistance due to their enhanced expression in various cancer types. Acting as efflux pumps, their overexpression in tumor cells promotes the active transport of drugs from the inside to the outside of the cell, reducing drug efficacy. In our preliminary results, both 5-FU and ETV were identified as substrates for both Pgp and BCRP, indicating a potential competition between the two drugs when administered concurrently. Hypothetically, if these proteins

are overexpressed in the PC-3 cell line, the drug with the highest affinity for the protein could be preferentially transported out of the cell, while the second drug (lower affinity) may not be pumped out. Consequently, the effectiveness of the second drug might increase. In the context of our study, since we observed that the combination of 5-FU and ETV produces the relevant cytotoxic effects on PC cells, we suggest that ETV may have a greater affinity for these proteins, allowing for the 5-FU anti-tumor effect. This potentially addresses challenges associated with chemotherapy resistance in tumor cells. Nevertheless, it is important to note that the expression of Pgp and BCRP proteins can vary not only among different types of cancer but also among individuals with the same cancer type. There is no clear information about their expression in PC-3 cell line. Additional studies should be conducted to explore the interaction between 5-FU and ETV at this level.

Considering the UM-UC-5 cells, the treated cells did not show very different morphologies compared to the control group. As the concentrations increased, the ETV-treated cells formed more vacuoles. The combination of the chemotherapeutic drug 5-FU and ETV had the same influence on the morphology of the UM-UC-5 cells. As the concentration of the ETV drug increased along with 13.41 μM of 5-FU, more vacuoles were visible in the cells. On the other hand, after 72 h of treatment, as the concentrations increased, the ETV-treated cells appeared slightly more elongated compared to the control. In the 72 h combination study, the treated cells appeared slightly more elongated compared to the control. Cells treated with 100 μM of ETV and 13.41 μM of 5-FU formed many vacuoles.

For these reasons, we can conclude that in the UM-UC-5 cells, ETV alone does not produce the expected effect, and neither did the combination. Thus, the repurposed drug ETV yields higher cytotoxicity in the prostate cell line than in the bladder, as observed in the combination studies as well.

5. Conclusions

The results from the UM-UC-5 cell line were not as expected and were different from those obtained in the prostatic tumor cells. ETV showed significant cytotoxic effects on the PC-3 cells, particularly because it is not its original therapeutic indication. Regarding the reference drug 5-FU, although it was not as effective as in other types of tumors, it managed to inhibit the viability of the PC-3 cells. On the other hand, it was possible to prove that the combination of 5-FU with ETV may be an advantageous association, surpassing the results of each drug alone, leading to a considerable decrease in PC-3 cell viability after 72 h exposure.

Based on the IC_{50} values obtained in this study, ETV appears to be more effective than 5-FU, as it exhibited a lower IC_{50} value. Regarding the combination studies, it is believed that there might have been a potentiation of 5-FU action by the repurposed drug ETV. Due to the promising results achieved with ETV in prostatic tumor cells and the potential associated mechanisms of action, it would be pertinent to consider testing this drug in other types of tumors, particularly those in which KDM5B is overexpressed (such as breast, lung, skin, liver, stomach, and colorectal, among others). We postulate that the most probable mechanism of action of ETV is through the inhibition of PARP, since PC may be associated with mutations in the BRCA1/2 genes. Therefore, we suggest extending studies to other cell lines that may be affected by these types of mutations, such as breast and ovarian cells.

In summary, drug repurposing has proven to be an effective strategy in PC treatment, as several candidates with characteristics optimizing existing treatments have been identified, saving time and money in investigating this cancer treatment. Particularly in this study, the utility of repurposing ETV in oncology has been demonstrated, notably through its combination with the reference drug 5-FU. However, further studies are necessary to ascertain the relevance of including ETV as a repurposed drug in clinical practice and to determine the efficacy and effectiveness of other potential candidates for oncological treatment. This emphasizes the need for personalized therapies tailored to each patient's and disease's characteristics.

Supplementary Materials: The following supporting information can be downloaded at: https://www.mdpi.com/article/10.3390/biomed4020015/s1, Figure S1: Morphological evaluations of PC-3 cells after exposure to increasing concentrations of 5-FU (0.01–100 μM) for 48 h. These results are representative of three independent experiments for 48 h. Control cells were treated with a concentration of 0.1% DMSO (vehicle). The scale bar is 50 μm; Figure S2: Morphological evaluations of PC-3 cells after exposure to increasing concentrations of ETV (0.01–100 μM) for 24, 48, and 72 h. These results are representative of three independent experiments for 24, 48, and 72 h. Control cells were treated with a concentration of 0.1% DMSO (vehicle). The scale bar is 50 μm; Figure S3: Morphological evaluations of PC-3 cells after exposure to the combination of the IC_{50} value of 5-FU (3.22 μM) with increasing concentrations of ETV (0.01–100 μM) added simultaneously and evaluated after 24, 48, and 72 h. These results are representative of three independent experiments for 24, 48, and 72 h. Control cells were treated with a concentration of 0.1% DMSO (vehicle). The scale bar is 50 μm; Figure S4: Morphological evaluations of UM-UC-5 cells after exposure to increasing concentrations of ETV (0.01–100 μM) for 24, 48, and 72 h. These results are representative of three independent experiments for 24, 48, and 72 h. Control cells were treated with a concentration of 0.1% DMSO (vehicle). The scale bar is 50 μm; Figure S5: Morphological evaluations of UM-UC-5 cells after exposure to the combination of the IC_{50} value of 5-FU (13.41 μM) with increasing concentrations of ETV (0.01–100 μM) added simultaneously and evaluated after 24, 48, and 72 h. These results are representative of three independent experiments for 24, 48, and 72 h. Control cells were treated with a concentration of 0.1% DMSO (vehicle). The scale bar is 50 μm.

Author Contributions: Conceptualization, N.V.; methodology T.L., L.M., E.R. and N.V.; formal analysis, T.L., L.M., E.R. and N.V.; investigation, T.L., L.M., E.R. and N.V.; resources, N.V.; writing—original draft preparation, T.L. and L.M.; writing—review and editing, N.V.; supervision, N.V.; project administration, N.V.; funding acquisition, N.V. All authors have read and agreed to the published version of the manuscript.

Funding: This research was financed by FEDER—Fundo Europeu de Desenvolvimento Regional funds through the COMPETE 2020—Operational Programme for Competitiveness and Internationalisation (POCI), Portugal 2020, and by Portuguese funds through Fundação para a Ciência e a Tecnologia (FCT) in the framework of the project IF/00092/2014/CP1255/CT0004 and CHAIR in Onco-Innovation at FMUP.

Institutional Review Board Statement: Not applicable.

Informed Consent Statement: Not applicable.

Data Availability Statement: Data are contained within the article and Supplementary Materials.

Acknowledgments: T.L., L.M. and E.R. acknowledge CHAIR in Onco-Innovation at FMUP for funding their supporting projects.

Conflicts of Interest: The authors declare no conflicts of interest.

References

1. Wong, V.K.; Ganeshan, D.; Jensen, C.T.; Devine, C.E. Imaging and Management of Bladder Cancer. *Cancers* **2021**, *13*, 1396. [CrossRef] [PubMed]
2. Oeyen, E.; Hoekx, L.; De Wachter, S.; Baldewijns, M.; Ameye, F.; Mertens, I. Bladder Cancer Diagnosis and Follow-up: The Current Status and Possible Role of Extracellular Vesicles. *Int. J. Mol. Sci.* **2019**, *20*, 821. [CrossRef] [PubMed]
3. Aveta, A.; Cilio, S.; Contieri, R.; Spena, G.; Napolitano, L.; Manfredi, C.; Franco, A.; Crocerossa, F.; Cerrato, C.; Ferro, M.; et al. Urinary MicroRNAs as Biomarkers of Urological Cancers: A Systematic Review. *Int. J. Mol. Sci.* **2023**, *24*, 10846. [CrossRef] [PubMed]
4. Saginala, K.; Barsouk, A.; Aluru, J.S.; Rawla, P.; Padala, S.A.; Barsouk, A. Epidemiology of Bladder Cancer. *Med. Sci.* **2020**, *8*, 15. [CrossRef] [PubMed]
5. Muscle-Invasive and Metastatic Bladder Cancer. Available online: https://uroweb.org/guidelines/muscle-invasive-and-metastatic-bladder-cancer/chapter/disease-management (accessed on 2 March 2024).
6. Hu, X.; Li, G.; Wu, S. Advances in Diagnosis and Therapy for Bladder Cancer. *Cancers* **2022**, *14*, 3181. [CrossRef] [PubMed]
7. Lourenço, T.; Vale, N. Pharmacological Efficacy of Repurposing Drugs in the Treatment of Prostate Cancer. *Int. J. Mol. Sci.* **2023**, *24*, 4154. [CrossRef] [PubMed]
8. Rawla, P. Epidemiology of Prostate Cancer. *World J. Oncol.* **2019**, *10*, 63–89. [CrossRef] [PubMed]

9. Bruno, S.M.; Falagario, U.G.; D'Altilia, N.; Recchia, M.; Mancini, V.; Selvaggio, O.; Sanguedolce, F.; Del Giudice, F.; Maggi, M.; Ferro, M.; et al. PSA Density Help to Identify Patients With Elevated PSA Due to Prostate Cancer Rather Than Intraprostatic Inflammation: A Prospective Single Center Study. *Front. Oncol.* **2021**, *11*, 693684. [CrossRef]
10. Cattrini, C.; Caffo, O.; Olmos, D.; Castro, E.; De Giorgi, U.; Mennitto, A.; Gennari, A. Apalutamide, Darolutamide and Enzalutamide for Nonmetastatic Castration-Resistant Prostate Cancer (NmCRPC): A Critical Review. *Cancers* **2022**, *14*, 1792. [CrossRef]
11. Currin, S.; Flood, T.A.; Krishna, S.; Ansari, A.; McInnes, M.D.F.; Schieda, N. Intraductal Carcinoma of the Prostate (IDC-P) Lowers Apparent Diffusion Coefficient (ADC) Values among Intermediate Risk Prostate Cancers. *J. Magn. Reson. Imaging* **2019**, *50*, 279–287. [CrossRef]
12. Pecoraro, M.; Del Giudice, F.; Magliocca, F.; Simone, G.; Flammia, S.; Leonardo, C.; Messina, E.; De Berardinis, E.; Cortesi, E.; Panebianco, V. Vesical Imaging-Reporting and Data System (VI-RADS) for Assessment of Response to Systemic Therapy for Bladder Cancer: Preliminary Report. *Abdom. Radiol.* **2022**, *47*, 763–770. [CrossRef] [PubMed]
13. Cancer. Available online: https://www.mayoclinic.org/diseases-conditions/cancer/diagnosis-treatment/drc-20370594 (accessed on 17 September 2023).
14. Prostate Cancer. Available online: https://uroweb.org/guidelines/prostate-cancer/chapter/treatment (accessed on 2 March 2024).
15. Zerbib, M.; Zelefsky, M.J.; Higano, C.S.; Carroll, P.R. Conventional Treatments of Localized Prostate Cancer. *Urology* **2008**, *72*, S25–S35. [CrossRef] [PubMed]
16. Knipper, S.; Ott, S.; Schlemmer, H.P.; Grimm, M.O.; Graefen, M.; Wiegel, T. Options for Curative Treatment of Localized Prostate Cancer. *Dtsch. Arztebl. Int.* **2021**, *118*, 228–236. [CrossRef] [PubMed]
17. Sayyid, R.K.; Klotz, L.; Benton, J.Z.; Ma, M.; Woodruff, P.; Satkunasivam, R.; Terris, M.K.; Wallis, C.J.D.; Klaassen, Z. Active Surveillance in Favorable Intermediate-Risk Prostate Cancer Patients: Predictors of Deferred Intervention and Treatment Choice. *Can. Urol. Assoc. J.* **2021**, *16*, E7–E14. [CrossRef] [PubMed]
18. Turanli, B.; Grøtli, M.; Boren, J.; Nielsen, J.; Uhlen, M.; Arga, K.Y.; Mardinoglu, A. Drug Repositioning for Effective Prostate Cancer Treatment. *Front. Physiol.* **2018**, *9*, 500. [CrossRef] [PubMed]
19. Duarte, D.; Vale, N. Antidepressant Drug Sertraline against Human Cancer Cells. *Biomolecules* **2022**, *12*, 1513. [CrossRef] [PubMed]
20. Pantziarka, P.; Verbaanderd, C.; Sukhatme, V.; Capistrano, R.; Crispino, S.; Gyawali, B.; Rooman, I.; Van Nuffel, A.M.; Meheus, L.; Sukhatme, V.P.; et al. ReDO_DB: The Repurposing Drugs in Oncology Database. *Ecancermedicalscience* **2018**, *12*, 886. [CrossRef] [PubMed]
21. Baraclude-Resumo Das Características Do Medicamento. Available online: https://www.ema.europa.eu/pt/documents/product-information/baraclude-epar-product-information_pt.pdf (accessed on 20 May 2023).
22. Entecavir. Available online: https://pubchem.ncbi.nlm.nih.gov/compound/Entecavir (accessed on 20 May 2023).
23. Lourenço, T.; Vale, N. Entecavir: A Review and Considerations for Its Application in Oncology. *Pharmaceuticals* **2023**, *16*, 1603. [CrossRef] [PubMed]
24. Jose, A.; Shenoy, G.G.; Rodrigues, G.S.; Kumar, N.A.N.; Munisamy, M.; Thomas, L.; Kolesar, J.; Rai, G.; Rao, P.P.N.; Rao, M. Histone Demethylase KDM5B as a Therapeutic Target for Cancer Therapy. *Cancers* **2020**, *12*, 2121. [CrossRef]
25. Ewert de Oliveira, B.; Junqueira Amorim, O.H.; Lima, L.L.; Rezende, R.A.; Mestnik, N.C.; Bagatin, E.; Leonardi, G.R. 5-Fluorouracil, Innovative Drug Delivery Systems to Enhance Bioavailability for Topical Use. *J. Drug Deliv. Sci. Technol.* **2021**, *61*, 102155. [CrossRef]
26. Pereira, M.; Vale, N. Repurposing Alone and in Combination of the Antiviral Saquinavir with 5-Fluorouracil in Prostate and Lung Cancer Cells. *Int. J. Mol. Sci.* **2022**, *23*, 12240. [CrossRef] [PubMed]
27. Rodrigues, D.; de Souza, T.; Coyle, L.; Di Piazza, M.; Herpers, B.; Ferreira, S.; Zhang, M.; Vappiani, J.; Sévin, D.C.; Gabor, A.; et al. New Insights into the Mechanisms Underlying 5-Fluorouracil-Induced Intestinal Toxicity Based on Transcriptomic and Metabolomic Responses in Human Intestinal Organoids. *Arch. Toxicol.* **2021**, *95*, 2691–2718. [CrossRef] [PubMed]
28. Fluorouracilo Accord-Resumo Das Características Do Medicamento. Available online: https://extranet.infarmed.pt/INFOMED-fo/index.xhtml (accessed on 20 May 2023).
29. Sethy, C.; Kundu, C.N. 5-Fluorouracil (5-FU) Resistance and the New Strategy to Enhance the Sensitivity against Cancer: Implication of DNA Repair Inhibition. *Biomed. Pharmacother.* **2021**, *137*, 111285. [CrossRef] [PubMed]
30. Calzetta, L.; Koziol-White, C. Pharmacological Interactions: Synergism, or Not Synergism, That Is the Question. *Curr. Res. Pharmacol. Drug Discov.* **2021**, *2*, 100046. [CrossRef] [PubMed]
31. Ribeiro, E.; Vale, N. Understanding the Clinical Use of Levosimendan and Perspectives on Its Future in Oncology. *Biomolecules* **2023**, *13*, 1296. [CrossRef] [PubMed]
32. MTT Assay Protocol for Cell Viability and Proliferation. Available online: https://www.sigmaaldrich.com/PT/en/technical-documents/protocol/cell-culture-and-cell-culture-analysis/cell-counting-and-health-analysis/cell-proliferation-kit-i-mtt (accessed on 30 July 2023).
33. Pires, D.E.V.; Blundell, T.L.; Ascher, D.B. PkCSM: Predicting Small-Molecule Pharmacokinetic and Toxicity Properties Using Graph-Based Signatures. *J. Med. Chem.* **2015**, *58*, 4066–4072. [CrossRef] [PubMed]
34. Fluorouracil. Available online: https://go.drugbank.com/drugs/DB00544 (accessed on 27 November 2023).
35. Daina, A.; Michielin, O.; Zoete, V. SwissADME: A Free Web Tool to Evaluate Pharmacokinetics, Drug-Likeness and Medicinal Chemistry Friendliness of Small Molecules. *Sci. Rep.* **2017**, *7*, 42717. [CrossRef] [PubMed]

36. Entecavir. Available online: https://go.drugbank.com/drugs/DB00442 (accessed on 27 November 2023).
37. Christians, U.; Schmitz, V.; Haschke, M. Functional Interactions between P-Glycoprotein and CYP3A in Drug Metabolism. *Expert Opin. Drug Metab. Toxicol.* **2005**, *1*, 641–654. [CrossRef] [PubMed]
38. Sikka, R.; Magauran, B.; Ulrich, A.; Shannon, M. Bench to Bedside: Pharmacogenomics, Adverse Drug Interactions, and the Cytochrome P450 System. *Acad. Emerg. Med.* **2005**, *12*, 1227–1235. [CrossRef]
39. Nebert, D.W.; Russell, D.W. Clinical Importance of the Cytochromes P450. *Lancet* **2002**, *360*, 1155–1162. [CrossRef]
40. Zhao, M.; Ma, J.; Li, M.; Zhang, Y.; Jiang, B.; Zhao, X.; Huai, C.; Shen, L.; Zhang, N.; He, L.; et al. Cytochrome P450 Enzymes and Drug Metabolism in Humans. *Int. J. Mol. Sci.* **2021**, *22*, 12808. [CrossRef] [PubMed]
41. Liu, X. Transporter-Mediated Drug-Drug Interactions and Their Significance. *Adv. Exp. Med. Biol.* **2019**, *1141*, 241–291. [PubMed]
42. Lin, J.H.; Lu, A.Y. Inhibition and Induction of Cytochrome P450 and the Clinical Implications. *Clin. Pharmacokinet.* **1998**, *35*, 361–390. [CrossRef] [PubMed]
43. Schwarzenbach, H. Predictive Diagnostics in Colorectal Cancer: Impact of Genetic Polymorphisms on Individual Outcomes and Treatment with Fluoropyrimidine-Based Chemotherapy. *EPMA J.* **2010**, *1*, 485–494. [CrossRef] [PubMed]
44. Park, J.Y.; Kim, K.A. Inhibitory Effect of 5-Fluorouracil on Human Cytochrome P450 Isoforms in Human Liver Microsomes. *Eur. J. Clin. Pharmacol.* **2003**, *59*, 407–409. [CrossRef] [PubMed]
45. Müller, F.; Fromm, M.F. Transporter-Mediated Drug-Drug Interactions. *Pharmacogenomics* **2011**, *12*, 1017–1037. [CrossRef] [PubMed]
46. BCRP/ABCG2 Substrates. Available online: https://go.drugbank.com/categories/DBCAT002663 (accessed on 27 November 2023).
47. Xu, Q.; Wang, C.; Meng, Q.; Liu, Q.; Sun, H.; Peng, J.; Ma, X.; Kaku, T.; Liu, K. OAT1 and OAT3: Targets of Drug-Drug Interaction between Entecavir and JBP485. *Eur. J. Pharm. Sci.* **2013**, *48*, 650–657. [CrossRef] [PubMed]
48. Mandíková, J.; Volková, M.; Pávek, P.; Navrátilová, L.; Hyršová, L.; Janeba, Z.; Pavlík, J.; Bárta, P.; Trejtnar, F. Entecavir Interacts with Influx Transporters HOAT1, HCNT2, HCNT3, but Not with HOCT2: The Potential for Renal Transporter-Mediated Cytotoxicity and Drug-Drug Interactions. *Front. Pharmacol.* **2016**, *6*, 304. [CrossRef] [PubMed]
49. Berrouet, C.; Dorilas, N.; Rejniak, K.A.; Tuncer, N. Comparison of Drug Inhibitory Effects (IC 50) in Monolayer and Spheroid Cultures. *Bull. Math. Biol.* **2020**, *82*, 68. [CrossRef] [PubMed]
50. Zhang, H.; Holden-Wiltse, J.; Wang, J.; Liang, H. A Strategy to Model Nonmonotonic Dose-Response Curve and Estimate IC50. *PLoS ONE* **2013**, *8*, e69301. [CrossRef]
51. FDA Antiviral Drug Advisory Committee Recommends Unanymously to Approve Entecavir for Hepatitis B. Available online: https://www.natap.org/2005/HBV/031505_02.htm (accessed on 15 September 2023).
52. Congregado, B.; Rivero, I.; Osmán, I.; Sáez, C.; López, R.M. PARP Inhibitors: A New Horizon for Patients with Prostate Cancer. *Biomedicines* **2022**, *10*, 1416. [CrossRef] [PubMed]
53. Branco, C.; Paredes, J. PARP Inhibitors: From the Mechanism of Action to Clinical Practice. *Acta Med. Port.* **2022**, *35*, 135–143. [CrossRef] [PubMed]
54. Center for Drug Evaluation and Research: Lonsurf (Trifluridine and Tipiracil). Available online: https://www.accessdata.fda.gov/drugsatfda_docs/nda/2015/207981Orig1s000PharmR.pdf (accessed on 15 September 2023).
55. Sun, W.; Sanderson, P.; Zheng, W. Drug Combination Therapy Increases Successful Drug Repositioning. *Drug Discov. Today* **2016**, *21*, 1189–1195. [CrossRef] [PubMed]